HHS Public Access

Author manuscript

Kidney Int. Author manuscript; available in PMC 2017 June 01.

Published in final edited form as:

Kidney Int. 2016 June ; 89(6): 1388–1398. doi:10.1016/j.kint.2016.02.004.

High-resolution renal perfusion mapping using contrast-enhanced ultrasound in ischemia-reperfusion injury monitors changes in renal microperfusion

Krisztina Fischer, MD, PhD[1,2], **F. Can Meral, PhD**[1], **Yongzhi Zhang, MD**[1], **Mark G. Vangel, PhD**[3], **Ferenc A. Jolesz, MD**[1], **Takaharu Ichimura, PhD**[2], and **Joseph V. Bonventre, MD, PhD**[2]

[1] Department of Radiology, Focused Ultrasound Laboratory, Brigham and Women's Hospital, Harvard Medical School, Boston, MA, USA

[2] Renal Division and Biomedical Engineering Division, Brigham and Women's Hospital, Harvard Medical School, Boston, MA, USA

[3] Department of Radiology, Massachusetts General Hospital, Harvard Medical School. Boston, MA, USA

Abstract

Alterations in renal microperfusion play an important role in the development of acute kidney injury with long-term consequences. Here we used contrast-enhanced ultrasonography as a novel method for depicting intra-renal distribution of blood flow. After infusion of microbubble contrast agent, bubbles were collapsed in the kidney and post-bubble destruction refilling was measured in various regions of the kidney. Local perfusion was monitored *in vivo* at 15, 30, 45, 60 minutes and 24 hours after 28 min of bilateral ischemia in 12 mice. High-resolution, pixel-by-pixel, analysis was performed on each imaging clip using customized software, yielding parametric perfusion maps of the kidney, representing relative blood volume in each pixel. These perfusion maps revealed that outer medullary perfusion decreased disproportionately to the reduction in the cortical and inner medullary perfusion after ischemia. Outer medullary perfusion was significantly decreased by 69% at 60 minutes post-ischemia and remained significantly less (40%) than pre-ischemic levels at 24 hours post-ischemia. Thus, contrast-enhanced ultrasonography with high-resolution parametric perfusion maps can monitor changes in renal microvascular perfusion in space and time in mice. This novel technique can be translated to clinical use in man.

Correspondence to: Ferenc A. Jolesz.

Corresponding Author: Joseph V. Bonventre M.D., Ph.D., Brigham and Women's Hospital, Harvard Institute of Medicine, Room 570, 4 Blackfan Circle, Boston, MA 02115, Phone: 617-525-5966, Fax: 617-525-5965 joseph_bonventre@hms.harvard.edu.

Disclosure

J.V.B and T.I. are co-inventors on KIM-1 patents that are assigned to Partners Healthcare and licensed by Partners to Johnson and Johnson, Sekisui, BiodenIdec, Astute, Novartis and a number of research reagent companies. The other authors have no personal financial or institutional interest in any of the drugs, materials, or devices described in this article.

Keywords

acute kidney injury; ischemia reperfusion

The pathophysiology of AKI involves tubular injury, inflammatory processes and changes in renal microvascular perfusion (1), which result in a generalized or localized impairment of oxygen and nutrient delivery to, and waste product removal from, cells of the kidney (2). The post-ischemia perfusion to the outer medulla is decreased disproportionately to the reduction in total kidney perfusion (3-6)) and likely in patients following ischemic injury (7). The local perfusion in the outer medulla can be reduced due to arteriolar vasoconstriction, endothelial injury, and local interstitial edema secondary to increased capillary permeability. This can result in tubular injury and interstitial inflammation which, in turn, can lead to decreased capillary density, chronic tissue hypoxia, and eventually fibrosis (6). Patients at risk for AKI often receive a combination of intravenous fluids and vasoconstrictive agents, which can further decrease local perfusion and increase interstitial edema (6). Therapeutic approaches, guided by impaired intra-renal perfusion and localized intra-renal edema, are not possible due to the absence of suitable bedside diagnostic and treatment monitoring technologies for detecting alterations and distributional deficiencies in renal microvascular perfusion.

Results and Discussion

We have applied contrast-enhanced ultrasonography (CEUS) to the assessment of the distribution of renal microperfusion in space and time in mice subjected to ischemiareperfusion injury (IRI) (8). While CEUS has been used to provide information regarding cortical perfusion (9-12), to our knowledge there is no CEUS study, which reliably demonstrates perfusion changes in the outer medulla. One reason why outer medullary perfusion could not be adequately assessed is interference with signals from large vessels. Another limitation of prior studies (13) is the use of reperfusion time to reach a % of quasi steady state blood flow. In AKI, when many outer medullary capillaries may be without flow, this parameter will not reliably reflect regional blood flow since the quasi steady state flow may be very impaired and yet the time to reach the % of that steady state flow unchanged.

In our study we used parasagittal transducer orientation, in which the large vessels are perpendicular to the imaging plane and do not disturb the visualization of the microvasculature in the outer medulla. In addition for data analysis we used plateau image intensity values. This reflects the actual microbubble delivery (microvascular blood flow) to the given location. During a 2-min intravascular infusion the microbubbles are collapsed using high MI ultrasound bursts and recovery is monitored over time in various regions of the kidney. High-resolution parametric perfusion maps were developed to detect and monitor microvascular perfusion changes in space and time, providing insight into the distributional changes in the microvascular perfusion, over space and time, in the kidney following IRI.

Mice were imaged at baseline and at various times after 28-min of bilateral ischemia with B-mode ultrasound. A dark region secondary to decreased echogenicity was present under the

kidney cortical area in images taken after 15 min of reperfusion (Figure 1). In the first hour after the clamp release this dark band became progressively less visible and at 60 min post-ischemia-reperfusion (post-IR) it was no longer apparent. The dark band was not seen in any pre-IR or 24 hr post-IR image or at any time point in control (sham) animals. There are two possible reasons for the brighter appearance of the post-IR cortical image: (1) The manipulation around the renal pedicles caused the elongation and modification of subcutaneous fat; (2) A small amount of contrast agent may remain from the first contrast infusion, although this is unlikely since the post-IR B-mode image was taken 43 min later [28 (ischemia duration) +15 (waiting time post-IR) = 43 min]. The half-life of the contrast agent is short (<5 min).

To estimate whole kidney and regional microvascular perfusion, high-resolution parametric perfusion maps of the kidneys were collected to detect distributional change in the microvascular perfusion. These are presented in pseudocolor (Figure 2A). While there was some variability among animals the perfusion maps clearly showed regional differences in microvascular perfusion of the post-IR kidney. The parametric maps revealed the most prominent perfusion loss in the outer medulla as early as 15 min after reperfusion (Figure 2A). The dark regions under the cortical region (outer medulla) that were found on B-mode images (Figure 1), reflecting reduced local perfusion, were located at the same regions on the parametric maps. On the 24 hr post-IR images delayed perfusion recovery persisted in the outer medulla. One animal, Mouse # IR7 developed more severe injury in response to the 28-min ischemia. The rapid and marked reduction in the microvascular perfusion can be identified on the parametric perfusion maps at post-IR 30-, 45-, and 60 min. This animal died post-IR 24 hr. No such spatial distributional change was found in any of the control animals (Figure 2A).

Representative single kidney perfusion tracings for the whole kidney (Figure 2B-C), or cortical, outer and inner medullary region (Figure 2D-E), were obtained for ischemic and control animals, by monitoring refill-induced non-linear signals of intact microbubbles after acutely collapsing them with high MI ultrasound bursts. After the removal of renal pedicle clamps, the microvascular perfusion gradually decreased in the whole kidney over the first hour post-IR (average perfusion decrease in the whole kidney was found as 50%, $p=0.0006$, $n=12$) as reflected by lower echo intensity plateau value at baseline at pre-burst and after burst. At 60 min post-IR perfusion was decreased in cortex and inner medulla but most in the outer medulla (by 69% compared to baseline pre-IR; $p=0.0001$). While cortical and inner medullary perfusion returned to levels close to baseline by 24 hr post-IR, outer medullary blood flow remained 40% ($p=0.0034$) reduced at 24 hr post-IR (Table 1). Total renal blood flow was decreased by 25% ($p=0.002$) at 24 hr post-IR. Furthermore the perfusion decrease was more significant ($p<0.0001$) at each time point post-IR in the outer medulla than in the cortex or inner medulla. There was approximately equivalent % reduction in cortical and inner medullary perfusion at various time points over the first 60 min after reperfusion. In control animals there were no significant spatial changes of perfusion in cortex, inner or outer medulla over time. Original Doppler and Contrast recordings of the control and IR kidneys are shown in Supplemental Videos 1-4.

To document post-ischemic kidney dysfunction and tissue injury we measured plasma creatinine, and performed histopathology and immunoperoxidase staining for Kidney Injury Molecule-1 (KIM-1) (Figure 3A). After 24 hr of reperfusion the serum creatinine increased significantly (from 0.2 ± 0.1 mg/dl at baseline to 2.0 ± 0.6 mg/dl, p=0.0009) with the range of 24 hr post-IR serum creatinine 1.3-2.9 mg/dl. KIM-1 expression, an established biomarker of renal proximal tubular injury (8), was greatly upregulated in the proximal tubules 24 hr post-IR by quantitative RT-PCR (Figure 3B). One day after IRI the level of normalized KIM-1 mRNA expression was increased by 40-180 fold in each animal. The KIM-1 mRNA expression levels (24 hr post-IR) correlated well (R=0.82, p=0.01, n=8) with the decrease in outer medullary image echo-intensity 60 min post-IR (Figure 3C).

Thus, in this study we have demonstrated that CEUS, coupled with our custom designed analysis algorithm, can effectively detect and monitor renal microvascular changes in space and time post-IRI in mice. The fact that our parametric perfusion maps indicated more severe ischemic injury in one of the IR animals (Mouse # IR7), which died post-IR 24 hr, further supports our method's reflection of the severity of AKI. Regional analyses and the perfusion maps indicated that microvascular perfusion recovery was delayed in the outer medulla, relative to the cortex and inner medulla. Histological analyses revealed the typical signs of IRI. There were no signs (e.g. interstitial hemorrhage), suggestive of cavitation effects induced by the microbubble disruption. These findings are in accordance with invasive studies (3-4), including recent ones by Ince and colleagues (14-17), revealing that the outer medulla has the largest deficit in microvascular perfusion after IRI. We found a dramatic perfusion decrease in the outer medulla between 30-, and 45 min post-IR, which was only partially resolved by 24 hr. These findings are in accordance with previous pathophysiology findings that the vasoconstriction, vascular congestion, small vessel occlusion, local edema and neutrophil infiltration develop very early (during the first hour post-IR) in AKI and persist in the outer medulla over the first 24 hr in ischemic animal models (1, 3, 18, 19).

CEUS is a readily available modality. The equipment is portable (bedside imaging is possible) and inexpensive. Testing is easily repeatable over time, and hence ideally applicable to the ICU setting. CEUS measurement is minimally invasive, requiring only an intravenous microbubble infusion. Studies have showed that CEUS can be used to reliably estimate renal perfusion in humans (9-12, 20). These prior studies, however, all presented the analysis of subjectively selected regions of interest in the kidney. To our knowledge, there is no previous study demonstrating the quantitation of medullary, especially outer medullary, microvascular perfusion in a reliable way using CEUS. The uniqueness of our study is the ability to provide information on the heterogeneous nature and spatial distribution of kidney local perfusion abnormalities in AKI through high-resolution, “pixel-by-pixel”, parametric perfusion maps. The regional perfusion discrepancies following IRI were detected as early as 15 min post-IR and lasted as long as 24 hr post-IR in each kidney. The observed decrease in relative blood perfusion in the outer medulla was significant at each examined time points despite the small number of animals studied. The ability to detect decreased intra-renal regional perfusion with CEUS in the clinical setting, has the potential to guide therapeutic decision making, especially with respect to vasoconstrictor agents and fluid therapies (3).

The results demonstrate that the described analysis methods can reliably detect microvascular perfusion changes in space and time. In this study isoflurane anesthesia was used, which has been previously associated with protective effect on the development of AKI in IRI via an anti-inflammatory process (21). Although injury was found in each animal, the isoflurane anesthesia may have reduced the extent of the injury. In addition, the relative blood volume, which was used to estimate the microvascular perfusion in each pixel, is not measured in a conventional unit, but rather as a perfusion estimation value, representing the local ultrasound contrast agent concentration. Since our results showed similar perfusion deterioration and partial recovery in each animal, we believe that the interpretation of the results is correct and can be easily applied to future clinical studies in man. CEUS can be used in a repetitive way at the ICU, to monitor intra-renal blood flow characteristics over time.

In conclusion, CEUS can be used to map renal microvascular perfusion heterogeneities at high-resolution in mice after an ischemic insult. This approach can be applied to humans and the resulting information can be used to monitor, at the bedside, the effects of the underlying disease state and guide personalized therapeutic interventions, including fluid treatment and vasoconstrictor agents. The perfusion maps might be particularly useful in sepsis or other states where vascular permeability is altered and interstitial edema may accumulate in the outer medulla affecting capillary blood flow to the S3 segment of the proximal tubule leading to the development of tubular injury. CEUS could also be useful in monitoring patients receiving nephrotoxic agents allowing early detection of drug-related renal regional ischemia.

Methods

The Complete Methods are available online as supplemental material.

Induction of AKI in mice

All experimental work was performed in accordance with the animal care and use protocol approved by the Institutional Animal Care and User Committee of the Harvard Medical School. Male BALB/c mice (n=12) were anesthetized with 1.2 % isoflurane in combination with compressed medical air and placed on a heated platform. The tail vein was catheterized for the contrast agent infusion. Body temperature and, heart rate were monitored with a built-in monitoring system of the ultrasound scanner (results are shown in Table 2). Once the kidneys were isolated the pre-IR image acquisitions were performed. Bilateral renal ischemia was induced by clamping both renal pedicles with non-traumatic microaneurysm clamps from a retroperitoneal approach for 28-min at 37.0 °C. After removal of the clamps, reperfusion of the kidneys was visually confirmed (8). The post-IR image acquisitions were then performed at 15-, 30-, 45-, 60 min and 24 hr post-IR. Animals were sacrificed 24 hr after the ischemic insult. Control (sham, n=3) animals were prepared and imaged over time, as the IR animals, but no renal ischemia was induced.

Image acquisition

Non-linear contrast imaging was performed with a Vevo 2100 (Visual Sonics, Toronto, Canada) ultrasound scanner and a 21 MHz linear transducer array. The ultrasound transducer was fixed in place with a mechanical positioning system, ensuring the constant position throughout the image acquisitions. Regular B-mode images were used to initially visualize the right kidney of the animal and to optimally position the imaging plane. A microbubble-based contrast agent (MicroMarker, Bracco, SpA, Italy) was injected with a syringe pump at the rate of 0.78 ml/hr for approximately 2-min. A destruction-reperfusion sequence was used. Non-linear contrast images were acquired based on the principle of amplitude modulation. Low mechanical index (MI) non-linear imaging mode was used until and ~20s after the contrast agent concentration reached the “steady state”. High MI “Burst” (MI=0.8, line density 512) pulses were delivered to destroy the contrast agents. Refilling was observed at low MI (MI=0.11, acquired at 25 Hz for 32 s). The image depth, focus gain, time gain compensation, and frame rate was optimized at the beginning of the study and was held constant in the experiments.

Image processing and analysis

Audio Video Interleave (AVI) files were acquired and processed on a personal computer using a non-linear time series analysis algorithm developed “in-house” in Matlab (The Mathworks, Natick, MA). Spectral analysis consists of a pixel-by-pixel Fourier transform approach in order to calculate the amount of ‘activity’ a certain image pixel experiences. The mask computed limited the region of interest (ROI) within the kidney tissue, excluding the major blood vessels. Intensities of the remaining pixels were fitted to an exponential perfusion model

In addition to the above pixel-by-pixel analysis, a similar non-linear curve fitting technique was applied to the manually selected ROI. The spatial average of each region was calculated and represented by a single curve. Three ROIs were chosen to be large enough to represent the cortex, outer-, and inner medulla. ROI selection was performed on parametric maps and confirmed on B-mode images and contrast images. The selected ROIs in the cortex, the outer medulla and the inner medulla were placed automatically on the consecutive images. (see more details in Complete Methods in Supplemental Material).

Renal functional parameter – plasma creatinine

A day before and 24 hr post-IR, a blood sample was collected from the animals. The plasma creatinine concentration was determined by the picric acid method, using a Beckman Creatinine Analyzer II.

Tissue collection, preparation and histology

Kidneys were perfused via the left ventricle with 0.9% saline solution at 37.0 °C until the kidney cortex completely cleared of blood. Kidneys were then removed immediately after the perfusion ended and either fixed and embedded in paraffin; or shock frozen. Paraffin sections were stained with H&E and PAS for histological examination. To demonstrate the tubular damage in response to the bilateral renal ischemia, immunohistochemical staining for KIM-1 was performed on alternate sections using goat polyclonal antibody (TIM-1/

KIM-1, catalogue number: AF1817, R&D Systems, Minneapolis, MN, USA) and a Vectastain Elite ABC kit (Vecor, Burlingame, CA, USA) was for visualization.

Quantification of KIM-1 mRNA by real-time quantitative reverse transcription PCR

Quantitative Real-Time-PCR (RT-PCR) analysis of mouse KIM-1 mRNA and 18S rRNA was performed as previously described (8). The following mouse KIM-1 primer set was used for the PCR, forward sequence: AGGAAGACCCACGGCTATTT, reverse sequence: TGTCACAGTGCCATTCCAGT. Each sample was measured three times.

Statistical analysis

A mix-model regression analysis was performed by using the “R” statistics package to fit the perfusion changes. For all the other statistical measurements the Student's t- test (SPSS 21 software (SPSS Statistics, IBM Corporation, Armonk, New York, USA)) was used. A P value of less than 0.05 was considered to be significant. Results are expressed as means ± S.D.

Supplementary Material

Refer to Web version on PubMed Central for supplementary material.

Acknowledgement

The study was founded by NIH grants DK 39773, DK72381 and R25 CA089017-06A2. We thank Visual Sonics (Toronto, Canada) for providing the MicroMarker contrast agent for this research project. The authors are very grateful to Fred Roberts and Dr. Sudeshna Fisch for their generous assistance during the experiments.

The preparation of this manuscript has been overshadowed by Dr. Jolesz’ sudden passing in December 2014. The main ideas and most of the composition of the paper were written jointly and we have done our best to complete them. In sorrow we dedicate this work to his memory.

References

1. Bonventre JV, Yang L. Cellular pathophysiology of ischemic acute kidney injury. J Clin Invest. 2011; 121(11):4210–21. [PubMed: 22045571]
2. Le Dorze M, Legrand M, Payen D, et al. The role of the microcirculation in acute kidney injury. Curr Opin Crit Care. 2009; 15(6):503–8. [PubMed: 19829106]
3. Mason J, Torhorst J, Welsch J. Role of the medullary perfusion defect in the pathogenesis of ischemic renal failure. Kidney Int. 1984; 26(3):283–93. [PubMed: 6513274]
4. Yamamoto K, Wilson DR, Baumal R. Outer medullary circulatory defect in ischemic acute renal failure. Am J Pathol. 1984; 116(2):253–61. [PubMed: 6465286]
5. Okusa MD, Jaber BL, Doran P, et al. Physiological biomarkers of acute kidney injury: a conceptual approach to improving outcomes. Contrib Nephrol. 2013; 182:65–81. [PubMed: 23689656]
6. Evans RG, Ince C, Joles JA, et al. Haemodynamic influences on kidney oxygenation: clinical implications of integrative physiology. Clin Exp Pharmacol Physiol. 2013; 40(2):106–22. [PubMed: 23167537]
7. Oostendorp M, de Vries EE, Slenter JM, et al. MRI of renal oxygenation and function after normothermic ischemia-reperfusion injury. NMR Biomed. 2011; 24(2):194–200. [PubMed: 20954164]
8. Yang L, Besschetnova TY, Brooks CR, et al. Epithelial cell cycle arrest in G2/M mediates kidney fibrosis after injury. Nat Med. 2010; 16(5):535–43. [PubMed: 20436483]

9. Kalantarinia K. Novel imaging techniques in acute kidney injury. Curr Drug Targets. 2009; 10(12): 1184–9. [PubMed: 19715540]
10. Schwenger V, Korosoglou G, Hinkel UP, et al. Real-time contrast-enhanced sonography of renal transplant recipients predicts chronic allograft nephropathy. Am J Transplant. 2006; 6(3):609–15. [PubMed: 16468973]
11. Schneider AG, Hofmann L, Wuerzner G, et al. Renal perfusion evaluation with contrast-enhanced ultrasonography. Nephrol Dial Transplant. 2012; 27(2):674–81. [PubMed: 21690200]
12. Schneider AG, Goodwin MD, Bellomo R. Measurement of kidney perfusion in critically ill Patients. Crit Care. 2013; 17(2):220. [PubMed: 23514525]
13. Kogan P, Johnson KA, Feingold S, et al. Validation of Dynamic Contrast-Enhanced Ultrasound in Rodent Kidneys as an Absolute Quantitative Method for Measuring Blood Perfusion. Ultrasound Med Biol. 2011; 37:900–908. [PubMed: 21601135]
14. Legrand M, Mik EG, Balestra GM, et al. Fluid resuscitation does not improve renal oxygenation during hemorrhagic shock in rats. Anesthesiology. 2010; 112(1):119–27. [PubMed: 19996951]
15. Aksu U, Demirci C, Ince C. The pathogenesis of acute kidney injury and the toxic triangle of oxygen, reactive oxygen species and nitric oxide. Contrib Nephrol. 2011; 174:119–28. [PubMed: 21921616]
16. Siegemund M, van Bommel J, Ince C. Assessment of regional tissue oxygenation. Intensive Care Med. 1999; 25(10):1044–60. [PubMed: 10551958]
17. Legrand M, Bezemer R, Kandil A, et al. The role of renal hypoperfusion in development of renal microcirculatory dysfunction in endotoxemic rats. Intensive Care Med. 2011; 37(9):1534–42. [PubMed: 21695476]
18. Farrar CA, Wang Y, Sacks SH, et al. Independent pathways of P-selectin and complement-mediated renal ischemia/reperfusion injury. Am J Pathol. 2004; 164(1):133–41. [PubMed: 14695327]
19. Park KM, Chen A, Bonventre JV. Prevention of kidney ischemia/reperfusion-induced functional injury and JNK, p38, and MAPK kinase activation by remote ischemic pretreatment. J Biol Chem. 2001; 276(15):11870–6. [PubMed: 11150293]
20. Hosotani Y, Takahashi N, Kiyomoto H, et al. A new method for evaluation of split renal cortical blood flow with contrast echography. Hypertens Res. 2002; 25:77–83. [PubMed: 11924730]
21. Lee HT, Ota-Setlik A, Fu Y, et al. Differential protective effects of volatile anesthetics against renal ischemia-reperfusion injury in vivo. Anesthesiology. 2004; 101:1313–1324. [PubMed: 15564938]

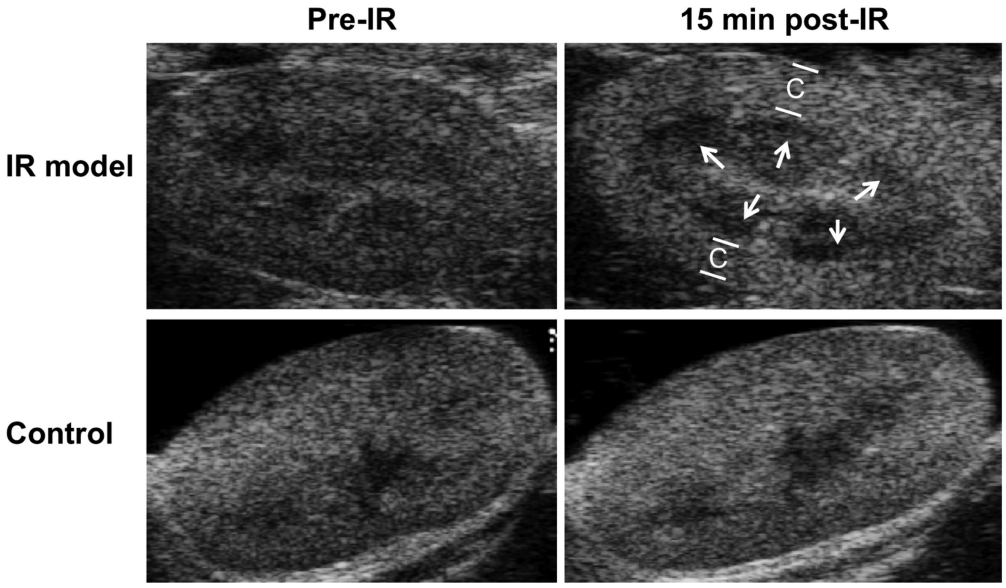

Figure 1. Brightness mode (B-mode) ultrasound images showed dark regions under the cortex 15 min post-IR

Male BALB/c mice were subject to 28-min of bilateral ischemia by clamping the renal pedicles. Animals were imaged with B-mode ultrasound at 15-, 30-, 45-, 60 min and 24 hr after reperfusion. At 15 minutes post-IR a dark region was found under the cortex (C) in the examined animals. The dark band was not seen in any pre-IR or 24 hr post-IR image. Control animals not exposed to IR did not show the dark band at any time point.

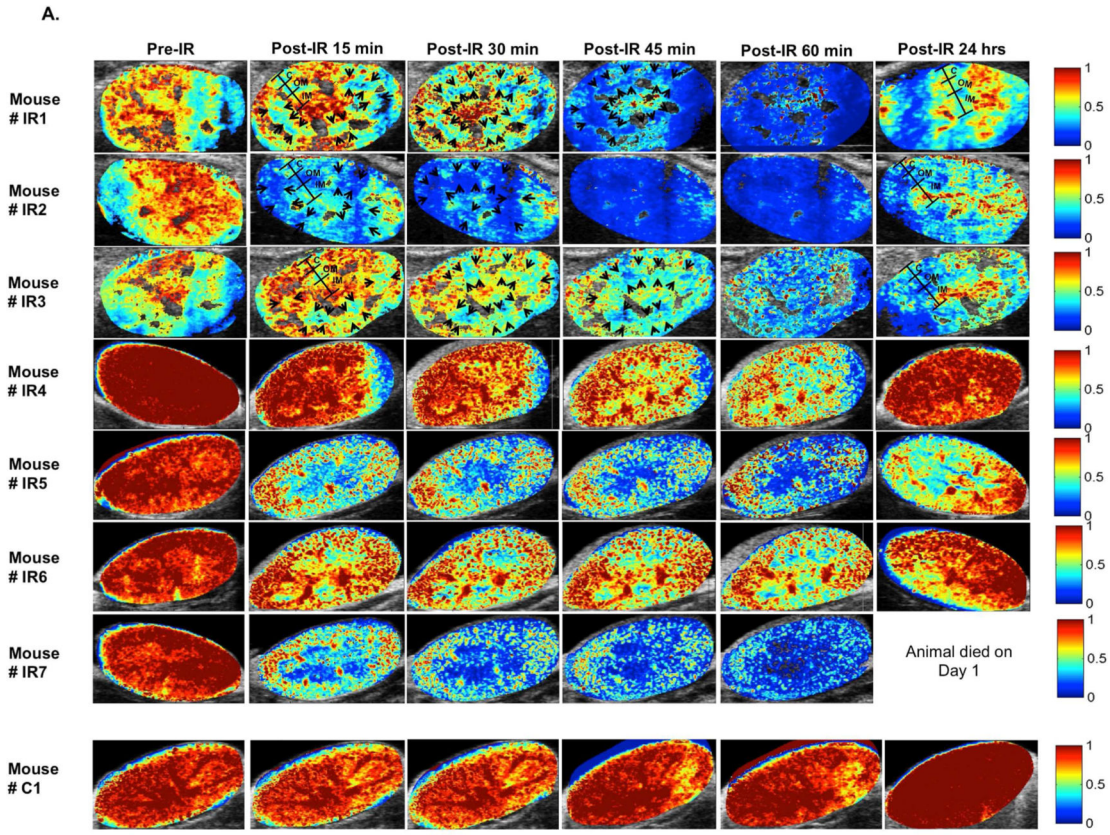

Figure 2A. High-resolution parametric perfusion maps of the kidney

Pre-IR, 15 min, 30 min, 45 min, 60 min and 24 hr post-IR perfusion maps of three animals' kidney are displayed in pseudocolor. Red and orange colors represent higher perfusion. On 15 min, 30 min and, in some cases, 45 min post-IR maps a noticeable blue band is visible under the cortical area (indicated by black arrows in Mouse # IR1-3), where the perfusion is substantially less than the other parts of the kidney. On 60 min post-IR maps the microvascular perfusion is significantly decreased in the entire kidney. The anatomical structures are indicated as C: cortex; OM: outer medulla; IM: inner medulla. Arcuate and interlobar arteries were localized as landmarks on the B-mode images, to distinguish between the cortex and the medulla. Note that on pre-IR images in mouse # IR1 and IR3 a large shadow was present and induced an artificial reduction in the signal intensity. This shadow was caused by the overlaying skin, which was identified on B-mode images. Please note that the Mouse # IR 4-7 were injected with a new batch of microbubbles, which gave stronger signal on the ultrasound imaging (which ultimately lead to a more intense "red" pseudocolor on the perfusion maps. High-resolution parametric perfusion maps of the control animal's kidney (Mouse # C1) are presented in the lowest row of the figure. Small time related changes in perfusion were similar in cortex, outer medulla and inner medulla.

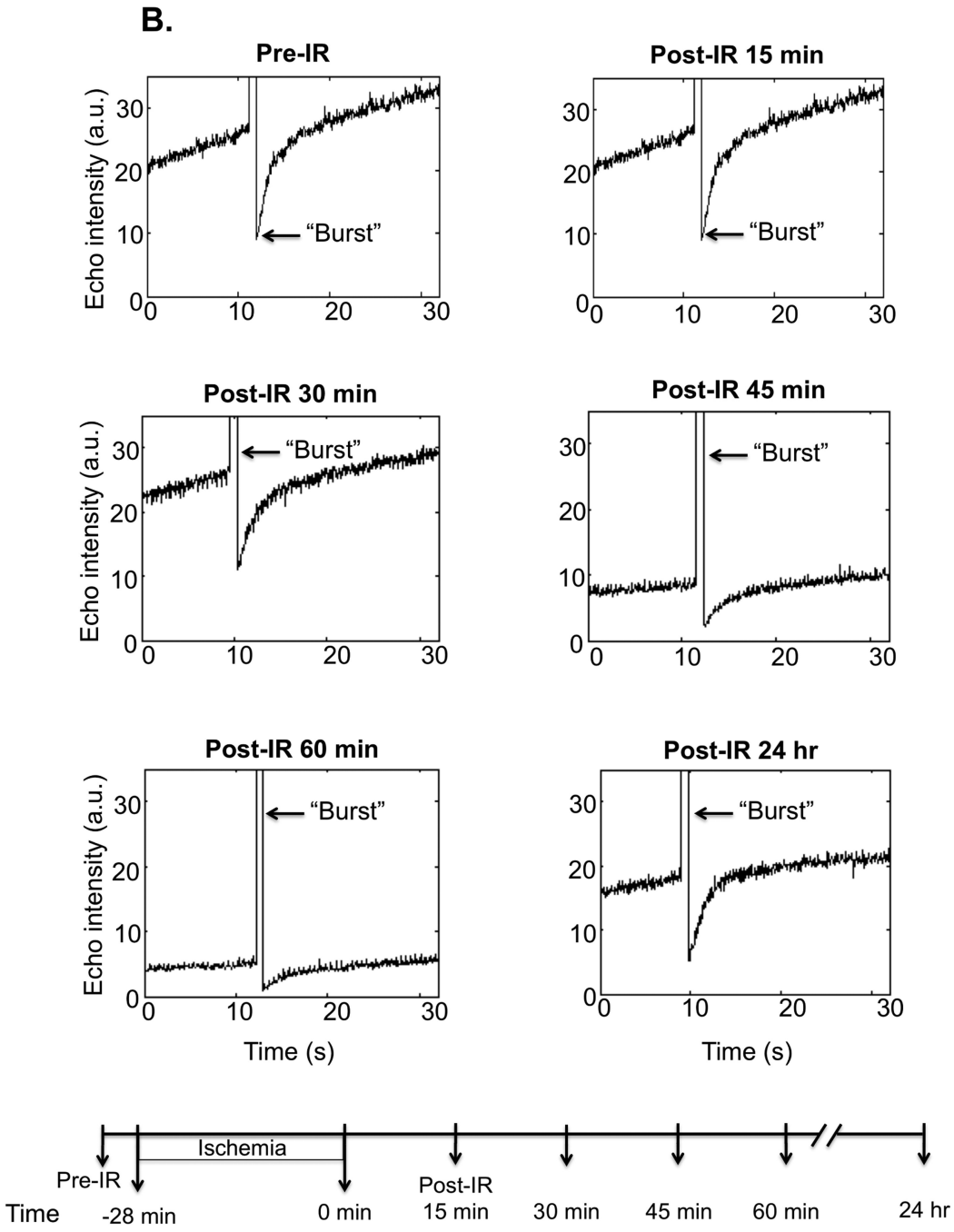

Figure 2B. Whole kidney perfusion curves based on refill sequence (after a high mechanical index "Burst"), example of one IR animal

Bubble refill contrast images were acquired at baseline, and at the beginning of each subsequent measurement as exemplified by a representative animal exposed to IR. The post-IR curves have a smaller plateau value and slower slope, indicating fewer and lower rate of restoration of bubbles in the post-ischemic kidney. The lower pre-"burst" echo intensity values, indicate lower steady state perfusion in the kidney at 45 and 60 min as well as 24 hr post-IR. This observation further confirms that the microvascular perfusion was declining in

the first hour post-IR. “Bursts” are indicated by arrows. The lower panel shows the timeline of the experiment.

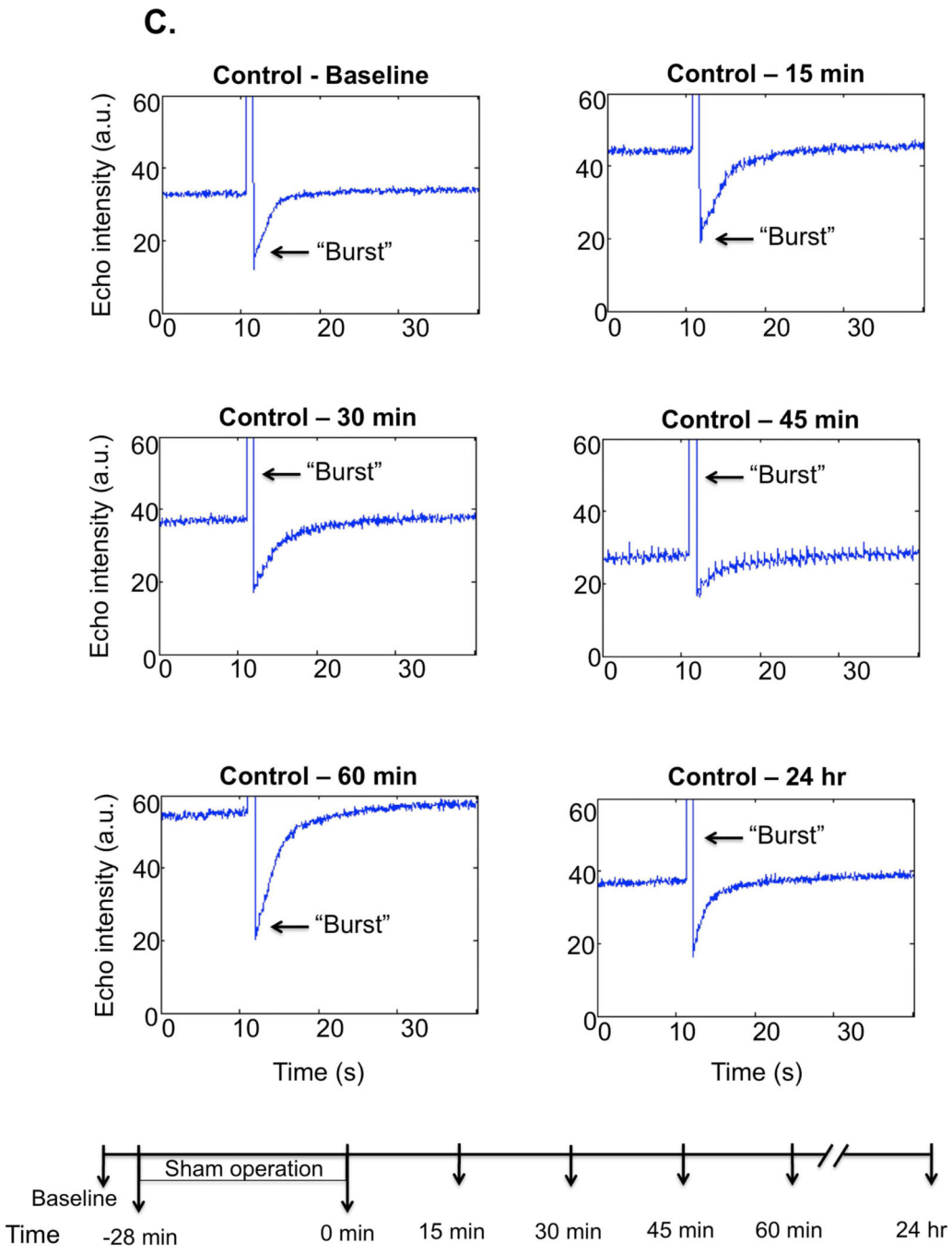

Figure 2C. Whole kidney perfusion curves of a control kidney

No major change was found in the whole kidney microvascular perfusion in the sham kidneys. The lower panel shows the timeline of the experiment.

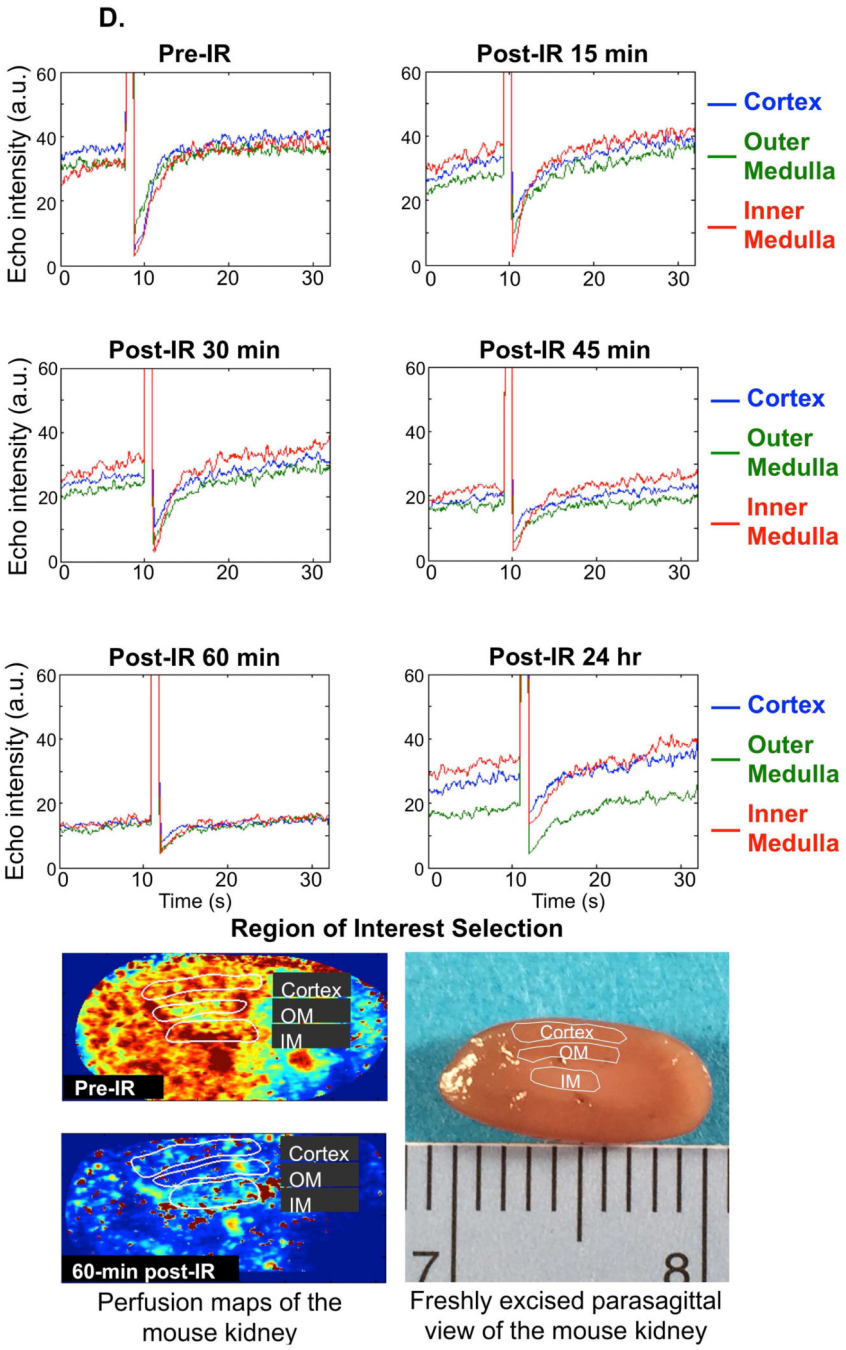

Figure 2D. Regional perfusion curves, example of one animal

The regional perfusion curves show that the microvascular perfusion decreased the most in the outer medulla during the first hour post-IR and its recovery took longer time compared to the cortex or to the inner medulla. Blue=cortex, Green=outer medulla, Red=inner medulla. Regions of interest selection on parametric maps and on B-mode images are shown in the lower panel of the figure. The region of interest selection was performed on the parametric perfusion maps (left panel) and confirmed on B-mode and contrast images at pre-IR, 15 min post-IR and 24 hr post-IR. The selected regions were maintained (placed automatically) on

consecutive images (15-, 30-, 45-, and 60 min post-IR). The right panel shows an overlay of the region selectioned onto a photograph of the freshly excised parasagittal view of the mouse kidney.

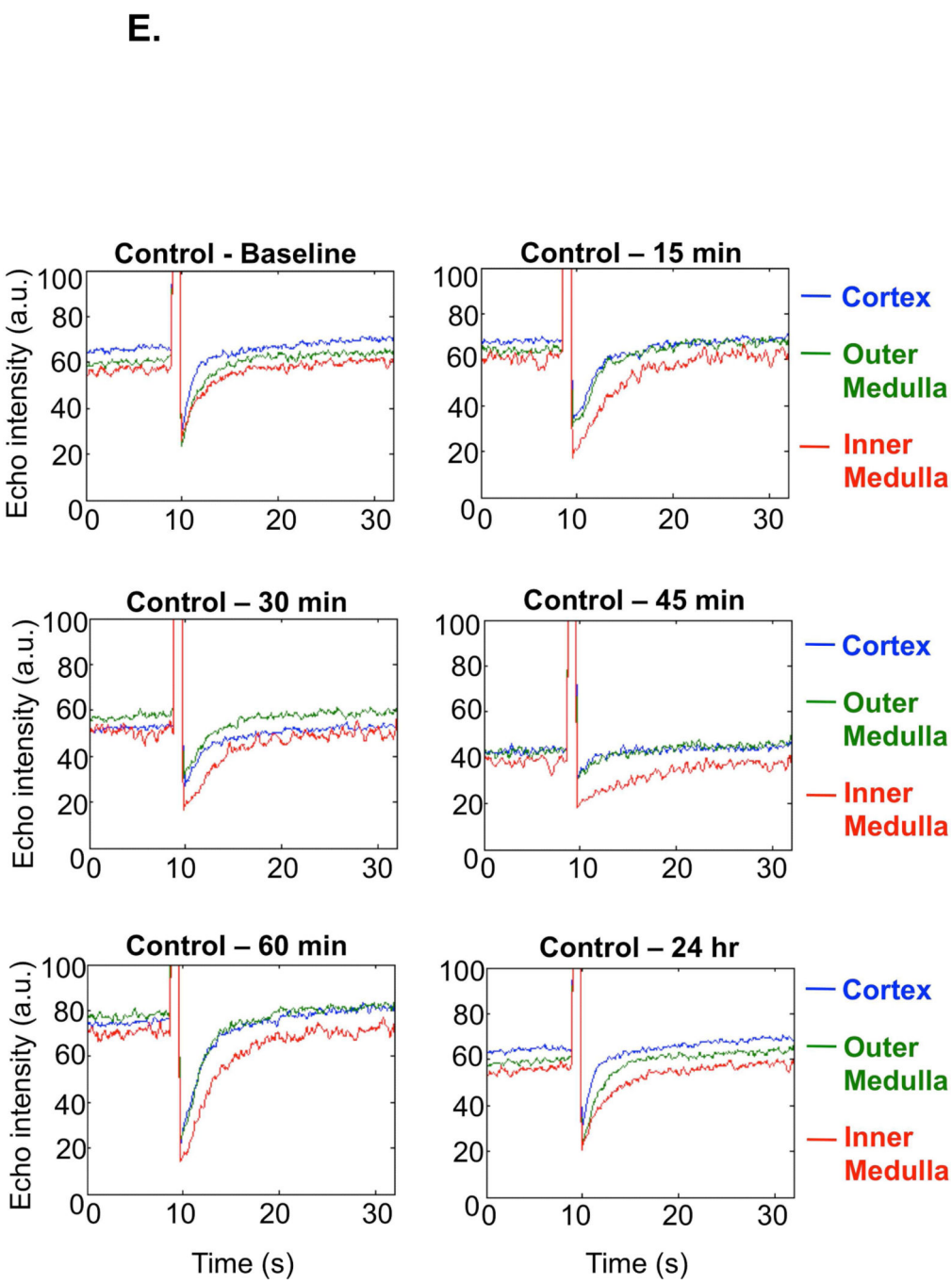

Figure 2E. Regional perfusion curves of the sham kidneys, example of one animal

No major change in regional perfusion was found in the sham kidney. Blue=cortex, Green=outer medulla, Red=inner medulla.

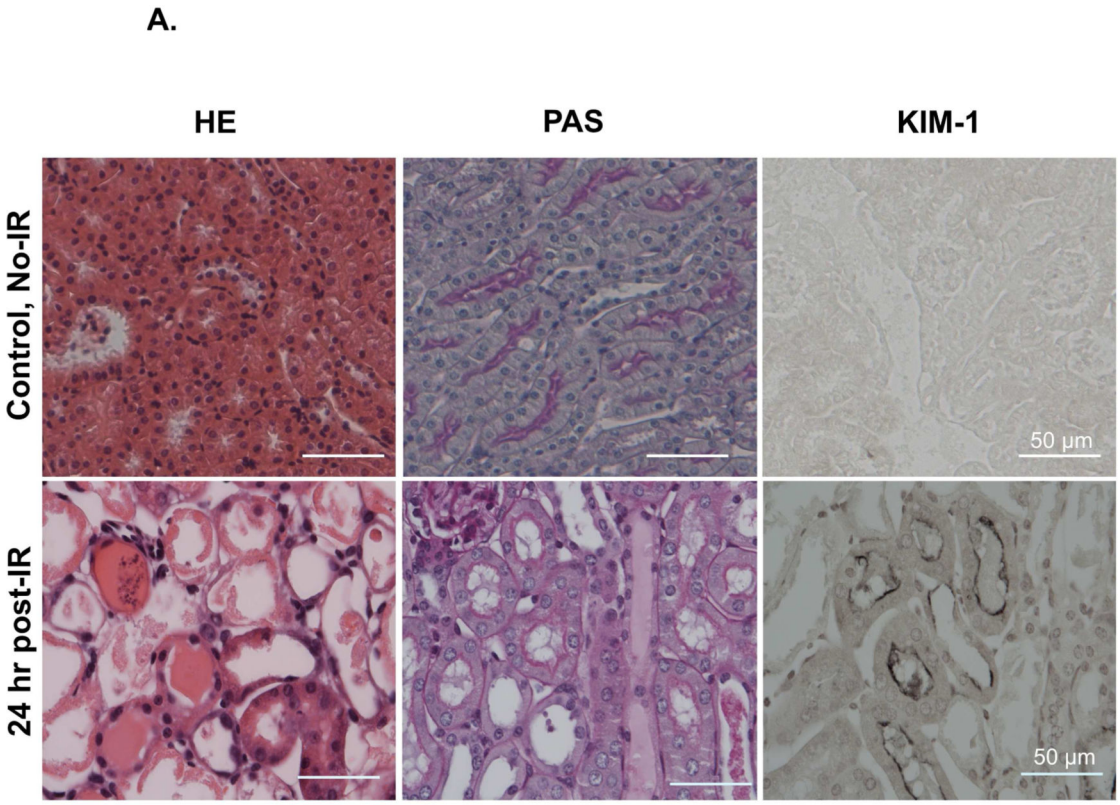

Figure 3A. Histology and Immunohistochemistry

Control (non-IRI) and IRI kidneys (24 hr reperfusion) were stained with Hematoxylin and Eosin staining (H&E), Periodic acid-Schiff (PAS) staining and KIM-1 immunostaining. H&E and PAS stained sections showed renal tubular damage, including proximal epithelial cell injury with loss of the brush border, necrosis, debris, cast formation in the tubular lumen space and tubular obstruction. KIM-1 staining was markedly upregulated in proximal tubules 24 hrs post-IR. Scale bar: 50 m.

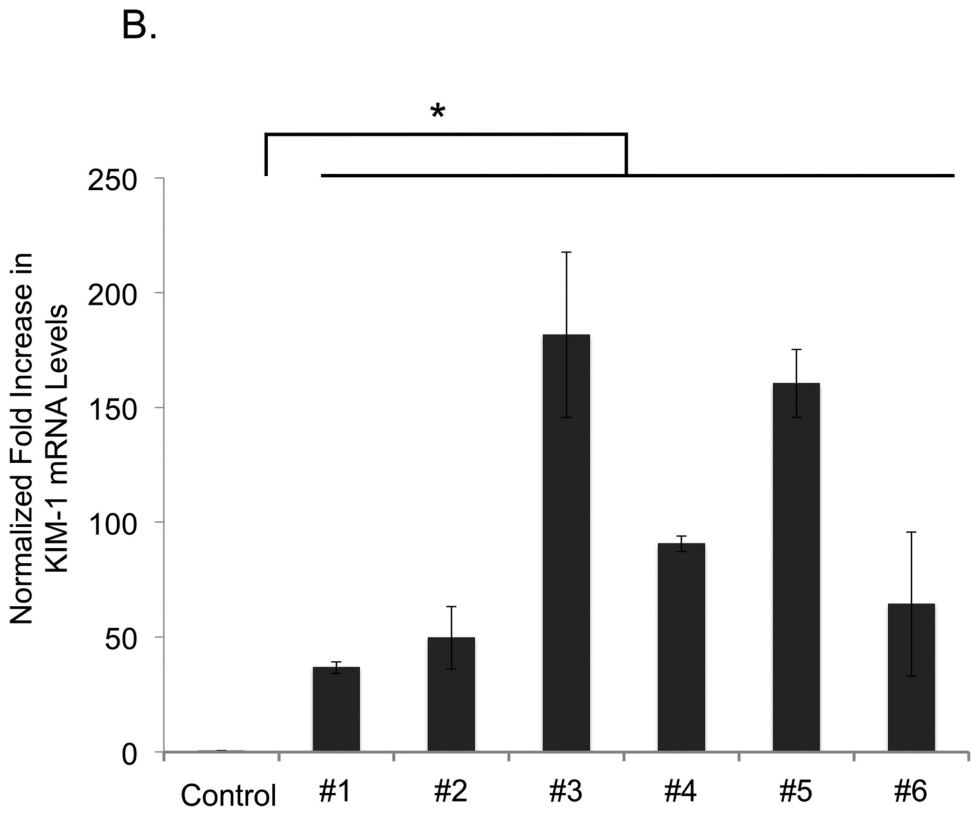

Figure 3B. Quantitative assessment of the renal injury

One day after the 28-min bilateral ischemia the average normalized KIM-1 expression level was 40-180 fold elevated compared to sham kidneys. Control= no IRI, #1- #6 = KIM-1 expression level in individual animals. * P<0.05.

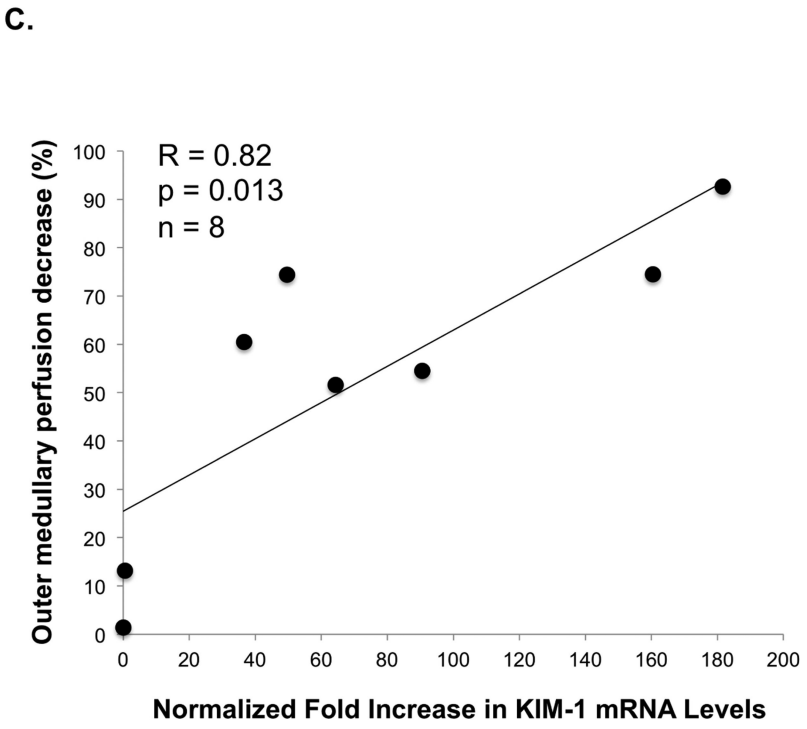

Figure 3C. Relationship between the decrease in outer medullary perfusion and KIM-1 mRNA expression

Correlation (R=0.82, p=0.013, n=8) was found between KIM-1 mRNA expression normalized to pre-IR mRNA levels and the outer medullary perfusion decrease 60 min post-IR. The outer medullary perfusion decrease was calculated from the outer medullary microvascular perfusion (plateau image intensity) at 60 min post-IR and plotted against normalized KIM-1 mRNA levels at 24 hr.

Kidney Int. Author manuscript; available in PMC 2017 June 01.

Table 1

Average regional plateau image intensity pre-, and post-ischemic injury at varying time points.

Cortex (n=12)	Pre-Ischemia	Post-IR 15-min	Post-IR 30-min	Post-IR 45-min	Post-IR 60-min	Post-IR 24-hr
Mean (SD)	48.81 (16.6)	38.57 (13.43)	34.36 (13)	29.2 (13.28)	24.65 (14.58)	37.56 (16.82)
Mean Δ (%)		− 21	− 29.6	−40.2	−49.5	−23
P (mean Δ)		0.0265	0.0079	00021	0.001	0.0911

Outer Medulla (n=6)	Pre-Ischemia	Post-IR 15-min	Post-IR 30-min	Post-IR 45-min	Post-IR 60-min	Post-IR 24-hr
Mean (SD)	46.27 (15.78)	26.02 (10.62)	24.32 (10)	19.48 (9.22)	14.55 (8.2)	27.55 (10.57)
Mean Δ (%)		−43.8	−47.4	−58	−69	−40.5
P (mean Δ)		0.0024	0.0018	0.0005	0.0001	0.0034

Inner Medulla (n=6)	Pre-Ischemia	Post-IR 15-min	Post-IR 30-min	Post-IR 45-min	Post-IR 60-min	Post-IR 24-hr
Mean (SD)	46.48 (15.66)	32.76 (12.4)	31 (12.43)	25.75 (11.1)	18.87 (11)	37.34 (13.17)
Mean Δ (%)		−29.5	−33.5	−44.6	−59.4	−19.7
P (mean Δ)		0.0230	0.0158	0.001	0.002	0.0407

Mean Δ = (1-Post-IR/Pre-IR)*100, change in the average plateau image intensity at various time points.

Table 2

Physiological parameters.

	IR model or Sham	The day of ischemic insult			24-hr Post-IR
		Pre-IR	During ischemia	Post-IR (first hour)	
Average Body Temperature (°C (SD))	IR (n=12) Sham (n=3)	37.9 (0.8) 38.3 (1.2)	37.7 (1.5) 38.6 (0.5)	37.8 (0.5) 38.6 (0.4)	37.9 (0.5) 38.5 (0.9)
Average Heart Rate (Beats per min (SD))	IR (n=12) Sham (n=3)	475 (48) 496 (58)	474 (38) 513 (26)	482 (36) 514 (25)	479 (46) 516 (31)
Average duration of the Experiments (min (SD))	IR (n=12) Sham (n=3)		116 (15) 110 (8)		32 (9) 34 (2)

Animal body temperature was maintained ≥ 37 °C throughout the experiments (mean temperature in °C ±SD). Average heart rate was stable throughout the experiments (mean value ± SD in beats per minute). Visualization of the kidney was possible in each experiment. The average duration of the experiment is shown on the day of the ischemic insult and on the following day (in minutes (SD)). The microbubble infusion and the ultrasound imaging were well tolerated in every animal.